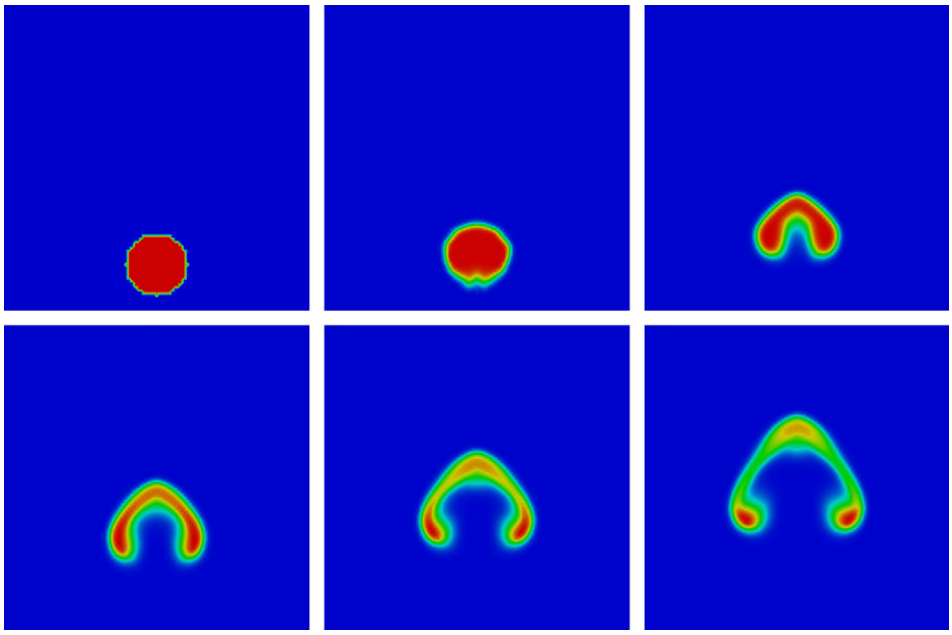

Fig. 2. Bubble ascension: isovalues of the volume fraction for the 100×100 mesh computation: classical upwind scheme.

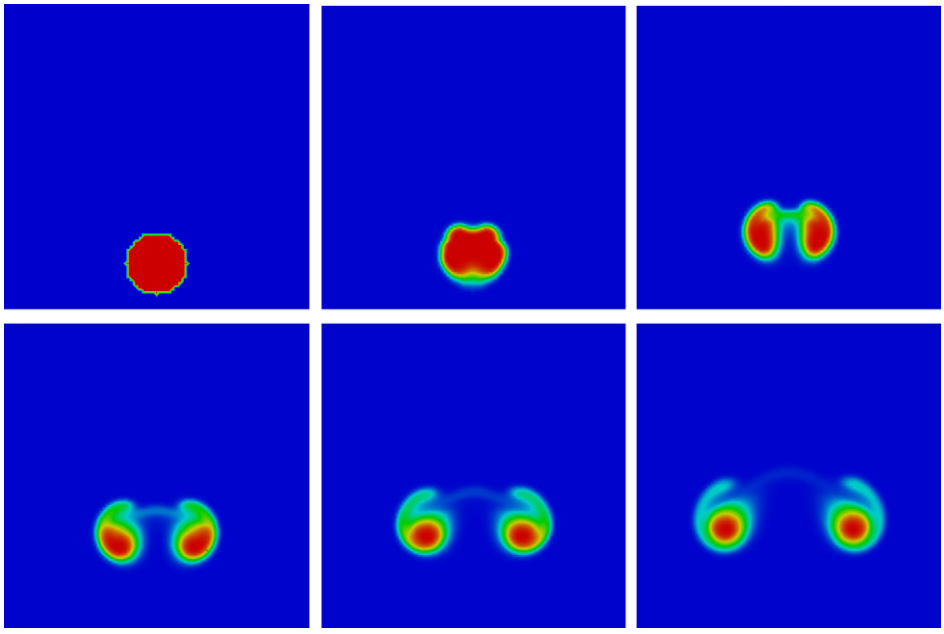

Fig. 3. Bubble ascension: isovalues of the volume fraction for the 100×100 mesh computation: preconditioned scheme with $\beta = 0.1$.

scheme. Namely, the time integration has used the three stage TVD Runge–Kutta discretization described in [11],

$$\begin{cases} \boldsymbol{Q}_i^{(1)} = \boldsymbol{Q}_i^n + \Delta t \mathbf{L}(\boldsymbol{Q}_i^n) & \text{(a)} \\ \boldsymbol{Q}_i^{(2)} = \frac{3}{4}\boldsymbol{Q}_i^n + \frac{1}{4}\boldsymbol{Q}_i^{(1)} + \frac{1}{4}\Delta t \mathbf{L}(\boldsymbol{Q}_i^{(1)}) & \text{(b)} \\ \boldsymbol{Q}_i^{n+1} = \frac{1}{3}\boldsymbol{Q}_i^n + \frac{2}{3}\boldsymbol{Q}_i^{(2)} + \frac{2}{3}\Delta t \mathbf{L}(\boldsymbol{Q}_i^{(2)}) & \text{(c)} \end{cases} \tag{57}$$

while the space discretization has used the MUSCL technique described in Section 3.3, with $\zeta = 1/3$ and the Spekreijse limiter. The results of this computation are shown in Fig. 4. Although the results of this fine mesh computation are not totally identical to those of Fig. 3, one can note the close similarity between these results and the one obtained with the preconditioned upwind scheme.

4.2. Broken dam problem

Here we present a computation of the well-known broken dam problem of Martin and Moyce [7]. Initially a water column with $a = 0.06$ m wide and $\eta^2 a = 0.12$ m high is a rest. Under the effect of the gravity $g = 9.81$ m s^{-2}, the column collapses. All the boundaries are solid walls. The

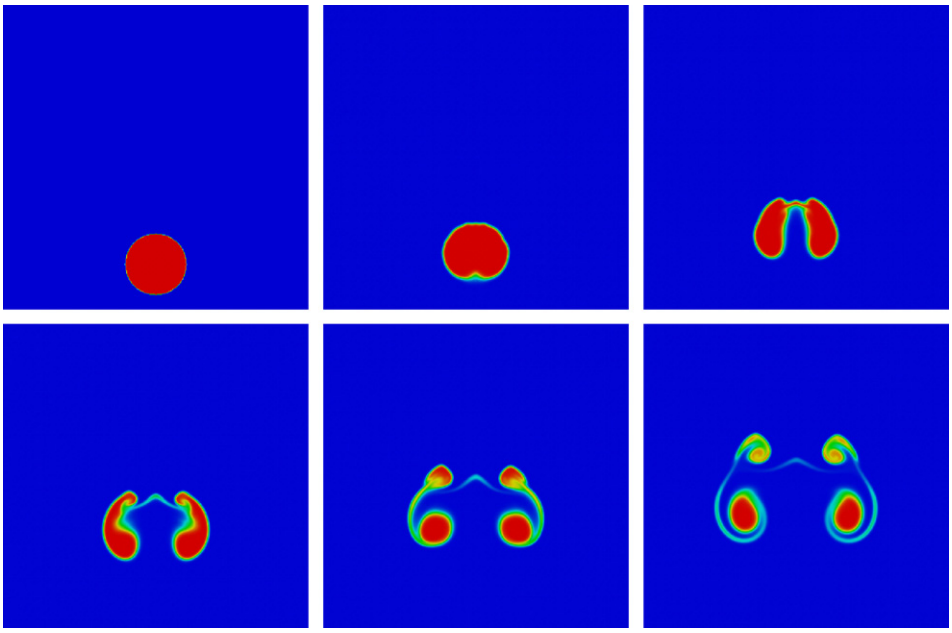

Fig. 4. Bubble ascension: isovalues of the volume fraction for the 400×400 fine mesh explicit computation.

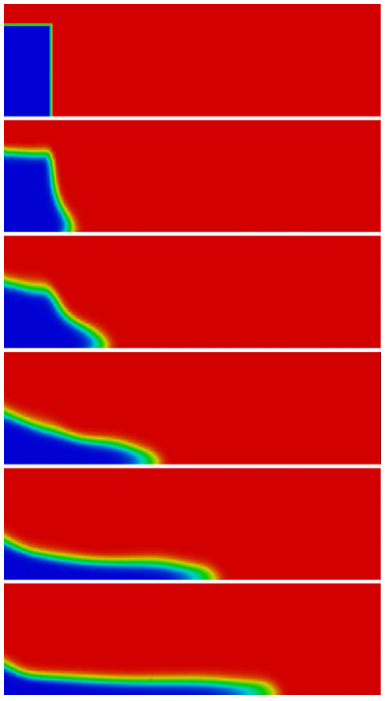

Fig. 5. Broken dam problem: isovalues of the volume fraction: classical upwind scheme.

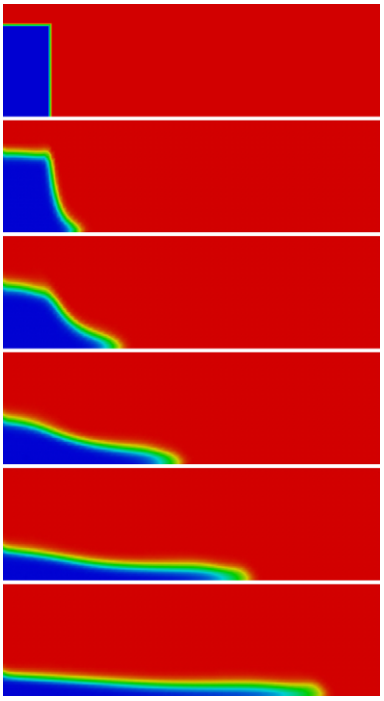

Fig. 6. Broken dam problem: isovalues of the volume fraction: preconditioned scheme with $\beta = 0.1$.

mesh we have used for this test, is regular with $\Delta_x = \Delta_z = 5 \times 10^{-3}$m. The Mach number during the computation is low and of the order of 1×10^{-1}. The implicit scheme has been used with a CFL number equal to 2.5 in order to compute with a sufficient accuracy the unsteady pattern of the flow. The linear system is solved by an iterative method with a linear residual $\theta = 1 \times 10^{-2}$. The space discretization has used the MUSCL technique with $\zeta = 1/2$ and the Van Albada–Van Leer limiter. We compute the solution with the standard and the preconditioned method. For the preconditioned method, the parameter of the Turkel's matrix β is chosen equal to 0.1 and remains constant in space and time.

Figs. 5 and 6 show the isovalues of the volume fraction at the different dimensionless times $t\sqrt{2g/a} = 0, 1.19, 1.98, 2.97, 4.02, 5.09$ corresponding to the physical

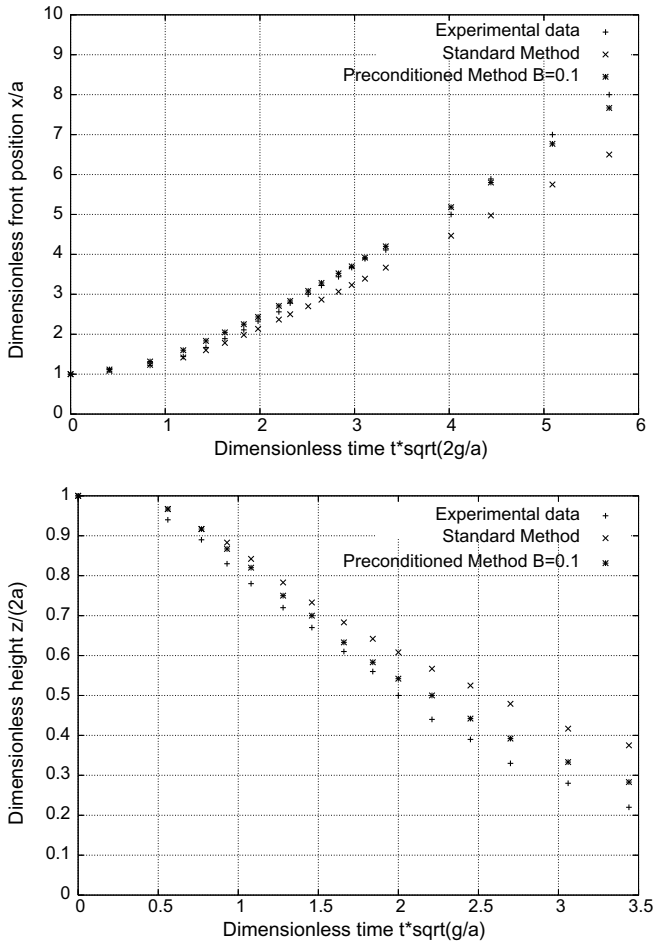

Fig. 7. Comparison between numerical solutions of the classical and preconditioned scheme and experimental results for the broken dam problem. Front position (top) and height of the column (bottom).

times $t = 0$, 0.066 s, 0.109 s, 0.164 s, 0.222 s, 0.281 s, for the standard (Fig. 5) and the preconditioned method (Fig. 6). It is clear that the upwind preconditioned scheme predicts a faster development of the flow and for instance the front position at time 0.281 s is clearly in advance with respect to the results obtained with the standard scheme.

To quantify the difference between the two schemes, we compare in Fig. 7, the two solutions with the experimental results of [7], for the front position $x/a = F_1\left(\eta^2, t\sqrt{2g/a}\right)$ and the height of the column $z/(\eta^2 a) = F_2\left(\eta^2, t\sqrt{g/a}\right)$. It is clear that the preconditioned method is more accurate than the standard one. For example at time $t\sqrt{2g/a} = 2.97$ the error compared to the experimental data for the front position is the order of 1% for the preconditioned method while it is the order of 10% for the classical upwind scheme.

4.3. Two-phase flow in a nozzle

Finally we present a sequence of computations of two-phase flows in a symmetric nozzle where the Mach number tends to zero. These computations are similar to the ones presented in [4] in single phase situation. The implicit scheme has been used with a CFL number equal to the inverse of the nonlinear residual of the mixture density $\mathrm{CFL} = 1/\mathrm{Res}(\rho)$ and at maximum equal to 10^6. The discrete solutions presented are the one obtained at convergence, i.e., for a residual equal to 10^{-9}. For the preconditioned method in this case, the parameter β is not taken as a constant but locally computed at each interface of the mesh and at each time step.

In these computations, an air–water two phase mixture defined by $(\alpha_1^\infty = 0.5, \rho_1^\infty = 1\ \mathrm{kg\ m^{-3}}, \rho_2^\infty = 1000\ \mathrm{kg\ m^{-3}})$ is injected in the nozzle with an horizontal imposed velocity equal to $u^\infty = 1\ \mathrm{m\ s^{-1}}$. The law states (56) for air and water are the same than previously and a representative Mach number of the flow is defined by

$$Ma_*^2 = \frac{(u^\infty)^2}{(\hat{a}^\infty)^2} = \frac{1}{(\hat{a}^\infty)^2} \tag{58}$$

Then the inlet pressure is taken as solution of equation $Ma_*^2 - 1/(\hat{a}^\infty)^2 = 0$ which can be rewritten using the equations of state of the two fluids:

$$Ma_*^2 - (\alpha_1^\infty \rho_1^\infty + (1-\alpha_1^\infty)\rho_2^\infty) \times \left(\frac{\alpha_1^\infty}{\gamma_1(p^\infty + \pi_1)} + \frac{1-\alpha_1^\infty}{\gamma_2(p^\infty + \pi_2)}\right) = 0 \tag{59}$$

We are interested in the situation where Ma_* tends to zero. In this case, the asymptotic analysis given in Section 2 applies and shows that the equations governing the flow are the two-phase incompressible Euler equations (14). Thus if we take at time $t = 0, \alpha_1(x,0) = 0.5$ for all x, we will get $\alpha_1(x,t) = 0.5$ for all x and $t > 0$ and (1) is simply the incompressible Euler equation with a constant density given by $(\rho_1 + \rho_2)/2$. We then expect that the limit solution of (1) will be given by an incompressible potential flow of density $(\rho_1 + \rho_2)/2$. In particular, the solution has to be symmetric with respect to the axis of the nozzle. To test the preconditioned scheme with respect to the classic non-preconditioned one, we realize three computations, respectively, at $Ma_* = 0.1, Ma_* = 0.01$ and $Ma_* = 0.001$.

Fig. 8 shows the isovalues of the normalized pressure $p - p_{\min}/p_{\max} - p_{\min}$ for the discrete stationary solutions obtained. Fig. 9 shows the profile of pressure in the upper and lower boundaries of the nozzle. We present from left to right the results obtained with the classical and the preconditioned scheme.

Fig. 9 shows clearly that the solution given by the classical discretization is not symmetric and consequently could not be a reasonable approximation of the incompressible solution. In addition, one can notice that the pressure fluctuations with the classic scheme (of order Ma_*) are larger than which obtained with the preconditioned one (of order Ma_*^2). To illustrate this difference in the behaviour of the pressure fluctuations, we plot in the first and second column of Fig. 9 the result for the classic and preconditioned method with the same pressure unit. We could note